Stability and nutrients removal performance of a Phanerochaete chrysosporium-based aerobic granular sludge process by step-feeding and multi A/O conditions

Lihui Cui, Hao Shen, Pengfei Kang, Xiaoying Guo, Haisong Li, Yan Wang, Junfeng Wan, Christophe Dagot

Stability and nutrients removal performance of a *Phanerochaete chrysosporium*-based aerobic granular sludge process by step-feeding and multi A/O conditions

Lihui Cui [a], Hao Shen [a], Pengfei Kang [a], Xiaoying Guo [a, c], Haisong Li [a, c], Yan Wang [a, c], Junfeng Wan [a, b*], Christophe Dagot [b, d]

[a] School of Ecology and Environment, Zhengzhou University, Zhengzhou 450001, PR China

[b] GRESE EA 4330, Université de Limoges, 123 avenue Albert Thomas, F-87060 Limoges Cedex France

[c] Henan International Joint Laboratory of Environment and Resources, Zhengzhou University, Zhengzhou 450001, PR China

[d] INSERM, U1092, Limoges, France

***Corresponding author:**

Junfeng Wan, E-mail address: wanjunfeng@zzu.edu.cn

Abstract

A *Phanerochaete chrysosporium*-based aerobic granular sludge (PC-AGS) was developed by inoculating fungal mycelial pellets into a lab-scale aerobic granular sequencing batch reactor (AGSBR). A strategy using step-anaerobic feeding coupled with multi A/O conditions was adopted. The results showed that the removal efficiencies for total phosphorus (TP) and total inorganic nitrogen (TIN) were 94.56 ± 2.92% and 75.20 ± 7.74%, respectively, under relatively low aeration time. Compared with original AGS, the content of extracellular proteins for PC-AGS obviously increased from 18.61 to 41.44 mg/g MLSS by the end of phase I. Moreover, the mature granules had a larger size and better stability during the 100 days operation. Furthermore, the analysis of microbial diversity detected many key functional groups in PC-AGS granules that were beneficial to nutrients removal. This work demonstrated that the addition of fungal pellets not only enhanced the removal performance, but also improved the stability of the AGS system.

Keywords: Aerobic granular sludge; Mycelium pellets; Nutrients removal; Stability

1. Introduction

Since aerobic granular sludge (AGS) technology was firstly reported in 1991, the formation mechanisms and application of aerobic granular sludge have become hot topics in the field of water treatment research (Mishima & Nakamura, 1991; Zhang et al., 2020). Compared with traditional activated sludges, AGS exhibits a denser structure, quicker settlement, higher pollutant removal performance, greater biomass enrichment, and higher resistance to load shock (Yan et al., 2019; Yuan et al., 2019). However, the main problems encountered when utilizing AGS is its instability, which limits its application in the wastewater treatment. The phenomenon of aerobic granular sludge disintegration was often reported after long-term operation, which leads to subsequent biomass loss and the final failure of AGS system (Liu et al., 2004; Schwarzenbeck et al., 2005). To address this instability, biological process with the potential to enhance granular stability and pollutant removal performance must be investigated.

Many studies aimed at improving the stability of AGS have been conducted, but most have focused on organic loading rate (OLR), C/N ratio, hydraulic selection pressure, substrate composition, temperature, and pH as determining factors (Corsino et al., 2017; Wang et al., 2018a; Yin et al., 2019a; Yuan et al., 2019). However, in actual practice, the operating conditions of reactors and characteristics of wastewater are difficult to adjust and change in real time. So, rather than actively responding to reactor or wastewater conditions, microbial attachment growth strategies have been applied as effective methods to decrease sludge loss and increase biomass production, which enhances sludge stability by adding biomass carriers (Wang et al., 2019; Zhang et al., 2020). In fact, mycelial pellets are a novel and eco-friendly biomass material that can combine other organisms and substances to form self-immobilized

bio-mixtures that have a good self-immobilization capacity, making them suitable biomass carriers for promoting aerobic granulation (Wang et al., 2019). Compared with other synthesized carriers, mycelial pellets could efficiently adsorb or remove pollutants from wastewater through physic-chemical reaction and biodegradation while not creating secondary pollution (Espinosa-Ortiz et al., 2016). Many studies have confirmed that fungi serve certain functions in sludge treatments, like degradation of refractory organic pollutants, nutrients (nitrogen and phosphorus) removal and can become fungal pellets (Dalecka et al., 2020; Espinosa-Ortiz et al., 2016). *Phanerochaete chrysosporium*, an infamous white rot fungus, has a high biosorption capacity and can produce enzymes that degrade various refractory and toxic organic compounds (Lu et al., 2009). Furthermore, it possesses an abundance of pores and a large specific surface area, which are conducive to the transfer of materials and oxygen (Wang et al., 2014). Although the mycelial pellets technology has good potential in wastewater treatment, especially for the removal of aromatic compounds (e. g. lignin), the real application of *Phanerochaete chrysosporium* mycelial pellets is rarely reported. Considering that the growth of bacteria is more competitive than that of fungi when treating real wastewater, it is necessary to investigate the influence of mycelial pellets on the classical AGS system.

Therefore, our study aimed to develop a strategy for the fast establishment of *Phanerochaete chrysosporium*-based aerobic granular sludge (PC-AGS) in a sequencing batch reactor (SBR) by inoculating white rot fungi *Phanerochaete chrysosporium* mycelium pellets into AGS. Meanwhile, the characteristics, performance, extracellular polymeric substances (EPS) content, and functional microorganisms of the mature granular consortia were observed over 100 days post-inoculation so as to clarify the possible mechanisms underlying this strategy. The

results from this study will help establish a feasible, eco-friendly, and simple strategy for full-scale applications.

2. Materials and methods

2.1. Preparation of mycelial pellets

Phanerochaete chrysosporium was inoculated into 100 mL liquid medium (mg/L) which consisted of glucose (10,000), ammonium tartrate (200), KH_2PO_4 (2000), $MgSO_4 \cdot 7H_2O$ (750), $CaCl_2$ (100), $CuSO_4$ (64), and TWEEN 80 (1000). Additionally, 20 mL of a trace element solution was added into 1000 mL of medium. The trace element solution (mg/L) contains: $MgSO_4$ (3000), $MnSO_4$ (500), 1 g/L NaCl (1000), 0.1 g/L $FeSO_4 \cdot 7H_2O$ (100), $CoCl_2$ (100), $AlK(SO_4)_2 \cdot 12H_2O$ (10), $ZnSO_4 \cdot 7H_2O$ (100), $Na_2MoO_4 \cdot 2H_2O$ (10) , and H_3BO_3 (10). *Phanerochaete chrysosporium* with prepared medium were incubated at 30°C with a constant rotary speed (150 rpm) for around 5 days until numerous mycelial pellets were formed.

2.2. AGS and synthetic wastewater composition

The selected original AGS (the mean size was 2650 μm) were cultivated in laboratory for more than 200 days. The initial concentration and the sludge volume index (SVI_{30}) of AGS in this experiment was approximately 7000 mg/L and 28 mL/g, respectively. The composition of the prepared synthetic wastewater (Table 1) included three organic carbon sources and each carbon source contributed 33% of the total COD (1000 ± 50 mg/L).

2.3. Reactor setup and operation

The experimental set-up consisted of a bioreactor with a working volume of 2 L (internal diameter = 5 cm and total height = 120 cm). The SBR was automatically

maintained at 25 ± 1°C. The influent was fed into the bottom of the reactor. The SBR was operated in 6 h cycles, each of which included three sub-cycles (115 × 3 = 445 min), the settling (5 min) and the discharging (10 min). Every internal cycle (115 min) included 10 min of anaerobic feeding with 0.23 L wastewater, 45 min of anerobic and 60 min of aeration. As shown in Table 2, the experimental period was divided into three phases (phase I, II, and III) according to the various nitrogen and phosphorus loading rates. Approximately 2 g (wet weight) of mycelial pellets with diameters ranging between 1–3 mm was added into the reactor at the start of each of the three phases.

2.4. Analytical methods

Water samples were regularly collected from the SBR system. The samples were immediately filtered through a 0.45 μm filter membrane and stored at 4°C. Chemical oxygen demand (COD), ammonia (NH_4^+-N), nitrite (NO_2^--N), nitrate (NO_3^--N), phosphate (PO_4^{3-}-P), sludge volume index after 30 (SVI_{30}) and 5 (SVI_5) minutes, MLSS, and MLVSS were measured in accordance with standard methods (APHA, 2005). Total inorganic nitrogen (TIN) was computed as the sum of NH_4^+-N, NO_2^--N, and NO_3^--N concentrations (Yan et al., 2019). The particle sizes of randomly selected granules (at least 100 granules for each sampling) were measured by the software of SEM image analysis (Nano Measurer System, 1.2.5). The morphology of the granular sludge samples was observed by digital camera and scanning electron microscopy (SEM, Zeiss/Auriga-bu, Germany). The aerobic granules were gathered from the bottom of SBR, then immediately washed three times with distilled water and dried at 105 °C for 24 h. After sulfuric acid-hydrogen peroxide digestion, the content of the total phosphorus (TP) was measured in accordance with standard methods (APHA, 2005). A heat extraction was applied to extract the EPS of the granular sludge

(Morgan et al., 1990). Then the concentration of polysaccharides (PS) and the protein (PN) in the EPS were quantified via the phenol-sulfuric acid method and the Lowry method (Dubios et al., 1956; Lowry et al., 1951).

2.5. Microbial community analysis

Sludge samples were extracted from the SBR reactor on days 34, 66, and 99, denoted as G1, G2, G3, respectively. DNA extraction, PCR amplification, and pyrosequencing were conducted sequentially using the general primers 338F (5'-ACTCCTACGGGAGGCAGCAG-3') and 806R (5'-GGACTACHVGGGTWTCTAAT-3') for bacteria following previously established procedures (Cheng et al., 2020). High-throughput sequencing was performed by Majorbio Bio-Pharm Technology Co. Ltd. (Shanghai, China) using the MiSeq PE300 platform (Illumina, USA) according to the manufacturer's instructions. The bioinformatics analysis was performed according to previously described methods (Cheng et al., 2020).

3. Results and discussion

3.1. Characterization of PC-AGS

3.1.1 Changes in morphology

The seed sludge was mainly characterized by a smooth outer surface with regular and dense structures with a mean size of 2650 μm. In phase II (100 mg/L NH_4^+-N), white filamentous organisms were observed growing on the surface of some granules. The aerobic granules with larger sizes usually had higher biomasses and richer microbial communities, resulting in an improved pollutant removal performance (Cui et al., 2019). However, the structures of large size aerobic granules were often unstable owing to the growth of filamentous bacterial (Xu et al., 2020). After phase II, the

biomass decreased rapidly due to the cracking and disintegration of granules, but the fragments were still large enough to be left in the reactor as a carrier for particle formation, as was also noted by Wang et al. (2014). At the same time, the white mycelial pellets with smooth surfaces roughened and turned gray after being inoculated into the reactor, probably owing to the adhesion of flocs. At the initial stage with the addition of MPs, two kinds of granular sludge including the original granular sludge and the granular sludge dominated by fungi could be easily separated in the system, while these two types eventually become one type of granular sludge named PC-AGS in the system at the steady period. PC-AGS had a dense structure that inhibited filamentous overgrowth under alkaline conditions, and a large number of intertwined filaments occupied the surface with many adsorbed cocci and bacilli. In fact, many cocci and bacilli cells could be attached to the surface and interior of MPs and some hyphae could adhere to the surface of granular sludge to promote the formation of microstructure pores or channels in the granules (Geng et al., 2020; Geng et al., 2021). Therefore, PC-AGS provided more surface area to absorb suspended solids and had many channels which could facilitate the transfer of nutrients and oxygen.

3.1.2 Biomass retention and granular settleability

MLSS and SVI are important parameters for evaluating the stability of AGS system. In phase I, due to disintegration, the flocculent sludge aggregated in PC mycelium pellets to form PC-AGS, and the MLSS had reached 9.50 g/L by day 34 (Fig. 1A). Previous research has reported that the microbial growth dominated by specific microorganisms was responsible for sludge granulation, and that the enhanced aggregation of microorganisms inside the flocs led to the formation of compact particles (Barr et al., 2010). The increases in influent nitrogen and phosphorus

concentration during phase II only resulted in decreases in the observed MLSS and MLVSS concentrations of PC-AGS between days 43 and 57 (from 12.60 and 8.05 g/L to 5.66 and 3.34 g/L for MLSS and MLVSS, respectively). The growth of filamentous fungi and bacteria was the primary reason for the change in biomass, and free fungi and flocs were washed away with the discharged effluents. Thereafter, after the microorganism had adapted to the changed environment, the MLSS and MLVSS concentrations of the PC-AGS continuously increased, gradually recovering to even higher levels despite the decreased influent ammonium concentration in phase III. In fact, the previous study showed that the classical AGS system without the addition of PCs was fragile and instable under step-feeding and multi A/O conditions (Cheng et al., 2020). Similarly, Geng et al. (2021) observed a loss of morphological integrity and deterioration of settling properties of the granules during prolonged operation without adding MPs. This indicated that using a microbial attachment growth strategy could greatly decrease sludge loss and increase biomass production for an AGS system (Zhang et al., 2020). During operation, the MLVSS/MLSS ratios decreased gradually (from 0.70 to 0.55), and were lower than those reported by Yin et al. (2019b). This low ratio was possibly due to the operational conditions (without regular discharge of the excess sludge for the PC-AGS system) and the abundant inorganic substances in the synthetic wastewater.

In contrast, a declining trend was observed for the SVI during the operation (Fig. 1B), indicating that the granular settleability of the PC-AGS system was gradually improving. SVI_{30} and SVI_5 decreased to their minimums (20.27 and 21.08 mL/g, respectively) on the 36th day, before they slightly increased, likely because of the decrease in MLSS that probably resulted from the competition between fungi and bacteria for nutrients. However, under operating conditions, SVI_{30} and SVI_5 recovered

207 rapidly and eventually stabilized in phase III at about 17 and 18 mL/g, respectively.
208 Moreover, the SVI values were always less than those of typical aerobic granules
209 which means the better settleability of PC-AGS (Liu & Tay, 2004). The overall
210 SV_{30}/SV_5 profile was increasing (Fig. 1B), and the maximum reached to 96% on the
211 36th day. Then, it stabilized above 90% for the remainder of the operational time,
212 which implied the stability of PC-AGS was better than traditionally AGS.

213 **3.1.3. Changes in EPS**

214 EPS secreted by microorganisms is mainly composed of PN and PS and is essential to
215 binding microbial aggregates together and guaranteeing the structural stability of
216 granules (Franca et al., 2018). The PS and PN contents and the ratios of PN/PS of the
217 three phases are shown in Fig. 1C. The initial PN content of the inoculated sludge was
218 low, but it gradually increased and eventually stabilized. These results were consistent
219 the previous report that revealed that PN changed the surface properties of granules
220 and promoted compact and stable aggregate structures (Yan et al. 2019). During the
221 phase II, the PN content obviously decreased when the ratio of COD:N was decreased
222 from 100:5 to 100:10, resulting in the PN/PS dropping from 2.53 to 1.58. The
223 decrease for the PN/PS ratio reflected the less negative charge and higher cell surface
224 hydrophobicity, which could probably result in increased instability of PC-AGS
225 (Zhang et al., 2007). Then, the flocculent sludge produced by the wastewater
226 gradually was aggregated to form new granules with the help of mycelial pellets,
227 which might be the reason for the increased EPS production in phase III (from 35.91
228 to 45.16 mg/g MLSS). The results of the EPS content analysis were consistent with
229 the changes in physical characteristics of the PC-AGS, which confirmed the
230 relationship between EPS content and granule structure proposed in previous studies
231 (Corsino et al., 2017). On the other hand, it should be pointed out that from the

Day-32 the PS content stabilized at 15.14 ± 1.58 mg/g MLSS, probably owing to the great quantity of PS content (41.28 ± 4.91 mg/g MLSS) secreted by *Phanerochaete chrysosporium*. It has been reported that PS may play a crucial role in microbial resistance to external pressure, and therefore, also in maintaining AGS stability (Xu et al., 2020; Yin et al., 2019a). Filamentous fungi can secrete a polymeric extracellular matrix (exopolysaccharides) that allows a growing colony to tenaciously adhere to substrates, owing to the formation of strong and multilayered coacervates (Harding et al., 2009). Furthermore, on day 69 in this study, the PS content in the outer layer of the PC-AGS was higher than that of the inner layer (25.86 ± 2.56 and 10.41 ± 0.84 mg/g MLSS, respectively), which greatly enhanced the granule strength (McSwain et al. 2005).

3.2. Performance of PC-AGS system

3.2.1. C, N, and P removal performance

COD and nutrients (nitrogen and phosphorus) removal efficiencies were analyzed during three phases (Fig. 2). PC-AGS contributed to high COD and phosphorus removal efficiencies (> 80% and > 90%, respectively) in phase I (Fig. 2A and B). The removal efficiencies of nitrogen and phosphorus for PC-AGS system showed an obvious decreasing trend when their influent concentrations increased to about 100 and 20 mg/L, respectively, which might have been related to the decrease in MLSS concentration. After a short period of adaptation, the removal efficiencies of COD and phosphorus of PC-AGS were increased to 94.37% and 90.13%, respectively, possibly due to the enhanced biomass retention. After 100 days operation, the average phosphorus content of PC-AGS (4.75 ± 0.08%, m/m) was higher than that of the conventional activated sludge, which was probably due to the accumulation of

256 phosphorus as the forms of hydroxyapatite (HAP) in the core of aerobic granules
257 (Zhang et al. 2013). In general, the changes in the COD and PO_4^{3-}-P removal
258 efficiencies were consistent with the variations in MLSS and MLVSS. It has been
259 reported that mycelial pellets can combine with other substances and organisms to
260 form compact particles and remove pollutants from wastewater via biosorbence and
261 biodegradation (Espinosa-Ortiz et al., 2016). In addition, Dalecka et al. (2020)
262 claimed that white rot fungi was able to remove phosphorus by biosorption and
263 metabolic activity. Therefore, PC-AGS might improve COD and PO_4^{3-}-P removal by
264 improving the environment for microorganisms.

265 The removal efficiencies of ammonium and TIN were monitored throughout the
266 long-term experiment. Initially, the removal efficiencies of ammonium and TIN were
267 low, and the effluent ammonium was above 17 mg/L on the first day (Fig. 2C). This
268 might have been because the sludge had not adapted to the new microenvironment.
269 Furthermore, the ammonium and TIN removal efficiencies in the PC-AGS system
270 were clearly affected by the C/N ratio. The influent had a constant COD concentration
271 (around 1000 mg/L) and the COD/N ratios of 20, 10, and 20 during the three phases,
272 which resulted in average effluent ammonium concentrations of 8.35 ± 3.03, 57.80 ±
273 11.23, and 13.28 ± 3.56 mg/L, corresponding to removal efficiencies of 83.39 ±
274 6.00%, 43.40 ± 10.92%, and 73.43 ± 6.97 %, respectively. These trends may be
275 explained by the relatively high free-ammonia (FA) concentrations, which may have
276 inhibited microbial activity. With the decrease in NH_4^+-N removal efficiency, the
277 granular structure was also adversely affected. Yang et al. (2004) observed that
278 aerobic granulation was negatively influenced when the concentration of FA was
279 more than 23.5 mg/L and the respiratory activity of nitrifying and heterotrophic
280 bacteria was reduced as FA risen from 2.5 to 39.6 mg/L. In addition, almost no

accumulation of nitrate or nitrite was observed for the duration of reactor operation (effluent nitrate and nitrite concentrations were less than 1.00 mg/L), indicating the removal rate of TIN was close to that of NH_4^+-N. Apparently, the alternation between aerobic and anaerobic conditions improved the denitrification process and achieved a much better TIN removal efficiency (Yuan et al., 2019). The phenomenon indicated that decreasing COD/N ratios had a harmful effect on ammonium removal, but had no influence on nitrate or nitrite removal in the PC-AGS system.

3.2.2. Kinetic study

In order to further analyze the mechanisms by which carbon, nitrogen, and phosphorus were simultaneously removed by PC-AGS, cyclic performance was examined at the end of each phase (Fig. 3). Compared with previous study (Gao et al., 2020), COD was not completely consumed until the end of the anaerobic stage, and then it decreased in the aerobic stage. This implied that COD was absorbed by anaerobic microorganisms to facilitate the phosphorus release in the anaerobic stage and denitrification in both anaerobic and aerobic stages. It is worth noting that PO_4^{3-}-P was released in the anaerobic phase, but then absorbed during the subsequent aerobic phase by polyphosphate accumulating organisms (PAOs). This process resulted in the PO_4^{3-}-P being removed from the system by the end of the aerobic cycle, implying that the PC-AGS had a stable enhanced biological phosphorus removal (EBPR) phenotype (Zhang et al., 2013). The extended anaerobic stage ensured efficient phosphorus removal, which may be the primary reason that the step feeding method had such an excellent and stable phosphorus removal efficiency (Wang et al., 2018a). In the meantime, the concentrations of phosphorus were higher in phase II and phase III (from 10.22 mg/L in phase I to 19.66 and 19.79 mg/L in phase II and phase III, respectively) matching the increase in influent phosphorus concentration, implying

306 that the activity of PAOs had been enhanced. This showed that the main mechanism
307 of phosphorus removal was biological phosphorus removal, and PC-AGS had higher
308 PAO activity when the step feeding strategy was applied.

309 Regarding nitrogen, the influent ammonium concentration was slightly delayed after
310 each feeding in phase II and phase III compared with phase I. This might have been
311 because a portion of the ammonium was initially absorbed by PC-AGS, but was
312 desorbed from the granules during feeding, which was consistent with the previous
313 results that showed a large portion of influent ammonium (30-40%) adsorbed by AGS
314 (Bassin et al., 2011). The PC-AGS exhibited a unique structure with channels and a
315 relatively large specific surface area, which means it contained an abundance of
316 interior adsorption sites (Wang et al., 2018b). However, the oxidation rate of
317 ammonium was remarkably low in the aerobic stage, which was possibly due to low
318 ammonia oxidizing bacteria (AOB) activity. Filamentous microorganisms can
319 consume large proportions of the DO, which might have an inhibitory effect on the
320 growth of AOB (Cheng et al., 2020). Meanwhile, the nitrite and nitrate concentrations
321 were very low throughout the whole cycle, but especially in phase II (< 0.5 mg/L),
322 thus demonstrating the excellent removal rate for TIN. An overall nitrogen loss
323 occurred since the accumulated nitrite and nitrate were less than the removed NH_4^+-N,
324 indicating that nitrification and denitrification (SND) occurred simultaneously in the
325 PC-AGS system (He et al., 2020). Furthermore, the alternating A/O condition with
326 step feeding at the beginning of each anaerobic phase could suppress the growth of
327 NOB and enrich the denitrifying PAOs (DNPAOs) (Ge et al., 2014). The nitrite
328 produced by AOB was probably denitrified immediately by denitrifying bacteria using
329 the internal carbon source in aerobic phase, which could help the enhancement of
330 phosphorus release and uptake in each sub-cycle (Fig. 3). These above-mentioned

results were confirmed by the subsequent analysis about microbial diversity and key functional genera.

3.3. Microbial population dynamics

3.3.1. Microbial diversity and richness

The diversity of the microbial communities were revealed using MiSeq pyrosequencing technology. The samples collected from phase I, phase II and phase IIII were denoted G1–G3, respectively, and a total of 52,983, 45,500, and 72,341 sequence reads were recovered, from which 290, 226, and 256 operational taxonomic units (OTUs) were identified. As shown in Table 3, the bacterial richness expressed by the least Chao1 index was the lowest when the ratio of COD/N was 10. However, there was little difference in the Shannon and Simpson estimators among samples. In phase II, bacterial death might have caused the decrease in microbial richness, but the microbial diversity was not obviously changed. It must be noted that, the plateaued rarefaction curves showed that the sequenced samples were an adequate representation of the population (Fig. 4A). As visualized in the Venn diagram (Fig. 4B), approximately 46% of the total OTUs were shared between the G1, G2, and G3 samples, indicating a continuous evolution of bacterial communities during the granulation of PC-AGS. Therefore, these results were in conformity to previous results, indicating that the richness and diversity of microbes is related to biomass concentration in PC-AGS systems and that the COD/N ratio could influence the bacterial richness of the microbial community.

3.3.2. Microbial community structure

The relative abundances and structures of the bacterial communities, at the phylum and family levels, in the granule samples with varying COD : N : P ratios are in Fig. 6. As shown in Fig. 5A, the seven phyla included Proteobacteria, Bacteroidetes, Actinobacteria, Chlorobi, Firmicutes, Chloroflexi, and Spirochaetes, of which Proteobacteria and Bacteroidetes were predominant in all samples, accounting for 88.31%, 81.27%, and 82.41% in samples G1–G3, respectively. These phyla have frequently been reported in activated and granular sludges (Zhang et al., 2020), implying these microbes are ubiquitous in biological wastewater treatment. Wang et al. (2011) found that Proteobacteria play an crucial role in organic and nitrogen removal, so they likely contributed to the PC-AGS pollutant removal performance. In addition, Proteobacteria can secrete large amounts of EPS which could help the adhesion of flocs to promote granulation (Liu et al., 2017). Bacteroidetes, which is a group of filamentous bacteria (Du et al., 2017), has the ability to degrade refractory organic compounds (Zhang et al., 2016), decreased from 12.82% (initial) to 6.93% and 8.89% in phase II and phase III due to the granulation process. Furthermore, the relative abundance of Chloroflexi dropped rapidly when influent conditions changed, while the relative abundances of Actinobacteria, Firmicutes, and Spirochaetae increased, especially if sample G1 is compared to sample G2, which implied that there was strong competition among these bacteria. Actinobacteria have been found to benefit sludge aggregation (Liu & Liu, 2006) and play an important nitrogen removal part in wastewater treatment systems (Farghaly et al., 2017). Firmicutes are a kind of carbohydrate fermenting bacteria which may also help with carbon consumption (Christy et al., 2014). Lee et al. (2013) reported that Spirochaetae accelerated the fermentation of amino acids and carbohydrates, making them a more consumable carbon source..

Seventeen genera with relative abundances greater than one percent were detected (Fig. 5B). Like observations at the phylum level, the genera with the highest relative abundance in the different samples were also different, *Thiothrix* in G1 (36.84%), *norank_f__norank_o__HOC36* in G2 (34.78%), and *Thiothrix* in G3 (34.85%). These differences might have been due to the changes in influent nitrogen concentration. *Thiothrix*, a filamentous bacterium that exhibits physiological activity under denitrification conditions and can reduce nitrate to nitrogen (Yang et al., 2018), mainly grew inside the granular structure. This can be used to explain why nitrate is removed so efficiently in the PC-AGS system throughout the operation. Conventional PAOs, i.e. *Candidatus_Accumulibacter*, were in the system, and were especially abundant in G2 (1.97%) when influent phosphorus concentration increased. In addition, some microorganisms with biological phosphorus removal abilities were also found, such as *Trichococcus* and *Desulfobulbus* (Guo et al., 2016), accounting for 0.04% and 0.54%, 3.11% and 0.47%, and 1.83% and 1.48% in the G1–G3 samples, respectively. Other dominant genera shared by G1–G3 included certain no-rank genera, some of which increased (e.g. *norank_f__Chlorobiaceae* and *norank_f__Propionibacteriaceae*) while others decreased (e.g. *norank_f__Saprospiraceae*, *norank_f__A4b*, and *norank_f__Veillonellaceae*). It has been reported that Propionibacteriaceae plays an important part in the biotransformation and biodegradation of various pollutants (Song et al., 2021). Chlorobiaceae has been frequently used in treating aniline wastewater, poultry slaughterhouse wastewater and pharmaceutical wastewater, etc. (Ma et al., 2020).

3.4.3. Key functional species

The key functional genera were categorized as ammonia-oxidizing bacteria (AOB), nitrite-oxidizing bacteria (NOB), denitrifying bacteria (DNB),

phosphorus-accumulating organisms (PAOs), denitrifying PAOs (DNPAOs), sulfate-reducing bacteria (SRB), and sulfide-oxidizing bacteria (SOB) to better assess the influence of microbial population dynamics on the performance of PC-AGS in simultaneously removing carbon, nitrogen, and phosphorus (Table 4).

Biological nitrogen and phosphorus removal was related to the microorganisms in the granules. Slow growing bacteria, especially PAOs, AOBs, and NOBs, have been shown to promote the stability of AGS (Franca et al., 2018). Specifically, nitrogen removal pathways consisted of denitrification, SND, and partial nitrification, which were related to the nitrifying and denitrifying bacteria. *Norank_f__Nitrosomonadaceae* were regarded as the predominant AOB, increasing slightly after an initial decrease (0.01-0.03%), while *Nitrospira*, *norank_f__Xanthomonadaceae*, and *norank_f__Pseudomonadaceae* were the identified NOB, decreasing from 0.65% to 0.10% in relative abundance. These trends indicated that the reduction in the ratio of COD/N was not conducive to the enrichment of AOB and NOB. On the other hand, at least 16 DNB were identified in the PC-AGS, indicating the DNB were diverse with high relative abundances and richness. In addition, the relative abundance of DNB (total) reduced from 38.88% to 30.49% with reduction COD/N ratio, and then returned to a high level (37.82%) when COD/N ratio returned to 20. The relatively high abundance of DNB in PC-AGS improved the removal efficiency of TIN. Competition between PAOs and GAOs is a main challenge, however, in this reactor the conventional GAOs, e.g. *Candidatus_Competibacter* and *Defluviicoccus*, were not detected, while PAOs, e.g. *Candidatus_Accumulibacter*, *Rhodococcus*, and *Acinetobacter*, were detected, possibly because of the extended anaerobic phase. These results were in conformity to He et al. (2018) who found that reduced aeration time inhibited the growth of GAOs

while promoting the growth of PAOs. During the operation, when influent phosphorus concentration increased to 20 mg/L the abundance of PAOs peaked at 2.09%. The presence of PAOs can ensure excellent PO_4^{3-}-P removal efficiency even in relatively low abundances (Gao et al., 2020), which is consistent with the performance of the reactor. DNPAOs can be important for PC-AGS formation and nitrogen and phosphorus removal (Yuan et al., 2019), and four identified DNPAOs, *Dechloromonas* (0.02–0.06%), *Hyphomicrobium* (0.08–0.37%), *Aeromonas* (0.07–0.15%), and *Comamonas* (0.00–0.17%), showed different tendencies in the three phases. Meanwhile, a complex microbial community composed of SOB and SRB was detected, especially in G3. Guo et al. (2016) found that SOB and SRB could have a synergistic effect on phosphorus release and phosphorus uptake, seemingly replacing the role of conventional PAOs. All these results further confirmed that mycelial pellets can provide favorable conditions for key functional groups that remove pollutants and promote the stability of PC-AGS.

4. Conclusions

In this study, a strategy to improve AGS stability and carbon, nitrogen, and phosphorus removal by adding *Phanerochaete chrysosporium* was proposed and tested. The results showed that PC-AGS maintained relatively high and stable carbon, nitrogen, and phosphorus removal efficiencies. The stable EPS production with increasing PN/PS ratios could ensure the long-term stability of PC-AGS. Moreover, PC-AGS had larger granules with many channels which facilitated a large number of functional microorganisms that could secrete more EPS and remove pollutants efficiently. The future research should be focus on the treatment of industrial wastewater containing refractory organic matter by PC-AGS.

Acknowledgements

The authors gratefully appreciated the financial support of Henan Provincial Science and Technology Development Program (Grant No. 212102110030), and the National Natural Science Foundation of China (Grant No. 21107100).

References

[1] APHA. 2005. *Standard methods for the examination of water and wastewater*. Washington, DC, USA.

[2] Barr, J.J., Cook, A.E., Bond, P.L. 2010. Granule Formation Mechanisms within an Aerobic Wastewater System for Phosphorus Removal. *Applied and Environmental Microbiology*, **76**(22), 7588-7597.

[3] Bassin, J.P., Pronk, M., Kraan, R., Kleerebezem, R., van Loosdrecht, M.C.M. 2011. Ammonium adsorption in aerobic granular sludge, activated sludge and anammox granules. *Water Research*, **45**(16), 5257-5265.

[4] Cheng, W.J., Zhang, L.G., Xu, W.J., Sun, Y.C., Wan, J.F., Li, H.S., Wang, Y. 2020. Formation and characteristics of filamentous granular sludge. *Water Science and Technology*, **82**(2), 364-372.

[5] Christy, P.M., Gopinath, L.R., Divya, D. 2014. A review on anaerobic decomposition and enhancement of biogas production through enzymes and microorganisms. *Renewable & Sustainable Energy Reviews*, **34**, 167-173.

[6] Corsino, S.F., Torregrossa, M., Viviani, G. 2017. The role of extracellular polymeric substances (EPS) on aerobic granules formation: comparison between a case of synthetic wastewater supply and another of industrial wastewater. *Desalination and Water Treatment*, **61**, 196-205.

[7] Cui, Y., Ravnik, J., Steinmann, P., Hribersek, M. 2019. Settling characteristics of nonspherical porous sludge flocs with nonhomogeneous mass distribution. *Water Research*, **158**, 159-170.

[8] Dalecka, B., Strods, M., Juhna, T., Rajarao, G.K. 2020. Removal of total phosphorus, ammonia nitrogen and organic carbon from non-sterile municipal wastewater with Trametes versicolor and Aspergillus luchuensis. *Microbiological Research*, **241**, 126586.

[9] Du, R., Cao, S.B., Li, B.K., Niu, M., Wang, S.Y., Peng, Y.Z. 2017. Performance and microbial community analysis of a novel DEAMOX based on partial-denitrification and anammox treating ammonia and nitrate wastewaters. *Water Research*, **108**, 46-56, 126586.

[10] Dubios, M., Gilles, K.A., Hamilton, J.K., Rebers, P.A., F., S. 1956. Colorimetric method for determination of sugars and related substances. *Analytical Chemistry*, **28**(3), 7.

[11] Espinosa-Ortiz, E.J., Rene, E.R., Pakshirajan, K., van Hullebusch, E.D., Lens, P.N.L. 2016. Fungal pelleted reactors in wastewater treatment: Applications and perspectives. *Chemical Engineering Journal*, **283**, 553-571.

[12] Farghaly, A., Enitan, A.M., Kumari, S., Bux, F., Tawfik, A. 2017. Polyhydroxyalkanoates production from fermented paperboard mill wastewater using acetate-enriched bacteria. *Clean Technologies and Environmental Policy*, **19**(4), 935-947.

[13] Franca, R.D.G., Pinheiro, H.M., van Loosdrecht, M.C.M., Lourenco, N.D. 2018. Stability of

aerobic granules during long-term bioreactor operation. *Biotechnology Advances*, **36**(1), 228-246.

[14] Gao, S.X., He, Q.L., Wang, H.Y. 2020. Research on the aerobic granular sludge under alkalinity in sequencing batch reactors: Removal efficiency, metagenomic and key microbes. *Bioresource Technology*, **296**, 122280.

[15] Ge, S., Peng, Y.Z., Qiu, S., Zhu, A., Ren, N. 2014. Complete nitrogen removal from municipal wastewater via partial nitrification by appropriately alternating anoxic/aerobic conditions in a continuous plug-flow step feed process. *Water Research*, **55**, 95-105.

[16] Geng, M.Y., Ma, F., Guo, H.J., Su, D.L. 2020. Enhanced aerobic sludge granulation in a Sequencing Batch Reactor (SBR) by applying mycelial pellets. *Journal of Cleaner Production*, **274**, 123037.

[17] Geng, M.Y., You, S.J., Guo, H.J., Ma, F., Xiao, X., Zhang, J.N. 2021. Impact of fungal pellets dosage on long-term stability of aerobic granular sludge. *Bioresource Technology*, **332**, 125106.

[18] Guo, G., Wu, D., Hao, T.W., Mackey, H.R., Wei, L., Lu, H., Chen, G.H. 2016. Granulation of susceptible sludge under carbon deficient conditions: A case of denitrifying sulfur conversion-associated EBPR process. *Water Research*, **103**, 444-452.

[19] Harding, M.W., Marques, L.L.R., Howard, R.J., Olson, M.E. 2009. Can filamentous fungi form biofilms? *Trends in Microbiology*, **17**(11), 6.

[20] He, Q.L., Chen, L., Zhang, S.J., Wang, L., Liang, J.W., Xia, W.H., Wang, H.Y., Zhou, J.P. 2018. Simultaneous nitrification, denitrification and phosphorus removal in aerobic granular sequencing batch reactors with high aeration intensity: Impact of aeration time. *Bioresource Technology*, **263**, 214-222.

[21] He, Q.L., Song, J.Y., Zhang, W., Gao, S.X., Wang, H.Y., Yu, J. 2020. Enhanced simultaneous nitrification, denitrification and phosphorus removal through mixed carbon source by aerobic granular sludge. *Journal of Hazardous Materials*, **382**, 121043.

[22] Lee, S.H., Park, J.H., Kang, H.J., Lee, Y.H., Lee, T.J., Park, H.D. 2013. Distribution and abundance of Spirochaetes in full-scale anaerobic digesters. Bioresource Technology, **145**, 25-32.

[23] Liu, J., Li, J., Wang, X.D., Zhang, Q., Littleton, H. 2017. Rapid aerobic granulation in an SBR treating piggery wastewater by seeding sludge from a municipal WWTP. *Journal of Environmental Sciences*, **51**, 332-341.

[24] Liu, Y., Liu, Q.S. 2006. Causes and control of filamentous growth in aerobic granular sludge sequencing batch reactors. *Biotechnology Advances*, **24**(1), 115-127.

[25] Liu, Y., Tay, J.H. 2004. State of the art of biogranulation technology for wastewater treatment. *Biotechnology Advances*, **22**(7), 533-563.

[26] Lowry, O.H., Rosebrough, N.J., Farr, A.L., Randall, R.J. 1951. Protein measurement with the Folin phenol reagent. *Journal of Biological Chemistry*, **193**(1), 265-75.

[27] Lu, Y., Yan, L.H., Wang, Y., Zhou, S.F., Fu, J.J., Zhang, J.F. 2009. Biodegradation of phenolic compounds from coking wastewater by immobilized white rot fungus Phanerochaete chrysosporium. *Journal of Hazardous Materials*, **165**(1-3), 1091-1097.

[28] Ma, K.L., Zhang, X.H., Shang, Y., Zhu, Z.K., Li, X.L., Li, X.L., Li, X.K. 2020. Improved purified terephthalic acid wastewater treatment using combined UAFB-SBR system: At mesophilic and ambient temperature. *Chemosphere*, **247**, 125752.

[29] McSwain, B.S., Irvine, R.L., Hausner, M., Wilderer, P.A. 2005. Composition and distribution of extracellular polymeric substances in aerobic flocs and granular sludge. *Applied and Environmental Microbiology*, **71**(2), 1051-1057.

[30] Mishima, K., Nakamura, M. 1991. Self-immobilization of aerobic activated-sludge: a pilot-study of the aerobic upflow sludge blanket process in municipal sewage treatment. *Water Science & Technology*, **23**(4), 981-990.

[31] Morgan, J.W., Forster, C.F., Evison, L. 1990. A comparative study of the nature of biopolymers extracted from anaerobic and activated sludges. *Water Research*, **24**(6), 743-750.

[32] Schwarzenbeck, N., Borges, J.M., Wilderer, P.A. 2005. Treatment of dairy effluents in an aerobic granular sludge sequencing batch reactor. *Applied Microbiology and Biotechnology*, **66**(6), 711-718.

[33] Song, T.W., Li, S.S., Yin, Z.C., Bao, M.T., Lu, J.R., Li, Y. 2021. Hydrolyzed polyacrylamide-containing wastewater treatment using ozone reactor-upflow anaerobic sludge blanket reactor-aerobic biofilm reactor multistage treatment system. *Environmental Pollution*, **269**, 116111..

[34] Wang, H.L., Li, P., Jin, Q.L., Qin, G. 2014. Specific aerobic granules can be developed in a completely mixed tank reactor by bioaugmentation using micro-mycelial pellets of Phanerochaete chrysosporium. *Applied Microbiology and Biotechnology*, **98**(6), 2687-2697.

[35] Wang, H.Y., Song, Q., Wang, J., Zhang, H., He, Q.L., Zhang, W., Song, J.Y., Zhou, J.P., Li, H. 2018a. Simultaneous nitrification, denitrification and phosphorus removal in an aerobic granular sludge sequencing batch reactor with high dissolved oxygen: Effects of carbon to nitrogen ratios. *Science of the Total Environment*, **642**, 1145-1152.

[36] Wang, L., Liu, X., Lee, D.J., Tay, J.H., Zhang, Y., Wan, C.L., Chen, X.F. 2018b. Recent advances on biosorption by aerobic granular sludge. *Journal of Hazardous Materials*, **357**, 253-270.

[37] Wang, L., Yu, T.M., Ma, F., Vitus, T., Bai, S.S., Yang, J.X. 2019. Novel self-immobilized biomass mixture based on mycelium pellets for wastewater treatment: A review. *Water Environment Research*, **91**(2), 93-100.

[38] Wang, X.H., Wen, X.H., Yan, H.J., Ding, K., Zhao, F., Hu, M. 2011. Bacterial community dynamics in a functionally stable pilot-scale wastewater treatment plant. *Bioresource Technology*, **102**(3), 2352-2357.

[39] Xu, J., Pang, H.L., He, J.G., Nan, J., Wang, M.F., Li, L. 2020. Start-up of aerobic granular biofilm at low temperature: Performance and microbial community dynamics. *Science of the Total Environment*, **698**, 134311.

[40] Yan, L., Zhang, M., Liu, Y., Liu, C., Zhang, Y. 2019. Enhanced nitrogen removal in an aerobic granular sequencing batch reactor under low DO concentration: Role of extracellular polymeric substances and microbial community structure. *Bioresource Technology*, **289**, 121651.

[41] Yang, S.F., Tay, J.H., Liu, Y. 2004. Inhibition of free ammonia to the formation of aerobic granules. *Biochemical Engineering Journal*, **17**(1), 41-48.

[42] Yang, Z.C., Yang, L.H., Wei, C.J., Wu, W.Z., Zhao, X.F., Lu, T. 2018. Enhanced nitrogen removal using solid carbon source in constructed wetland with limited aeration. *Bioresource Technology*, **248**, 98-103.

[43] Yin, Y.J., Liu, F.Y., Wang, L., Sun, J. 2019a. Overcoming the instability of aerobic granular sludge under nitrogen deficiency through shortening settling time. *Bioresource Technology*, **289**, 121620.

[44] Yin, Y.J., Sun, J., Liu, F.Y., Wang, L. 2019b. Effect of nitrogen deficiency on the stability of aerobic granular sludge. *Bioresource Technology*, **275**, 307-313.

[45] Yuan, Q., Gong, H., Xi, H., Xu, H., Jin, Z.Y., Ali, N., Wang, K.J. 2019. Strategies to improve aerobic granular sludge stability and nitrogen removal based on feeding mode and substrate.

Journal of Environmental Sciences, **84**, 144-154.

[46] Zhou, D.D., Liu, M.Y., Gao, L.L., Shao, C.Y., Yu, J. 2013. Calcium accumulation characterization in the aerobic granules cultivated in a continuous-flow airlift bioreactor. *Biotechnology Letters*, **35**(6), 871-877.

[47] Zhang, D.Y., Vahala, R.K., Wang, Y., Smets, B.F. 2016. Microbes in biological processes for municipal landfill leachate treatment: Community, function and interaction. *International Biodeterioration & Biodegradation*, **113**, 88-96.

[48] Zhang, H.L., Fang, W., Wan, Y.P., Sheng, G.P., Zeng, R.J., Li, W.W., Yu, H.Q. 2013. Phosphorus Removal in an Enhanced Biological Phosphorus Removal Process: Roles of Extracellular Polymeric Substances. *Environmental Science & Technology*, **47**(20), 11482-11489.

[49] Zhang, L.L., Feng, X.X., Zhu, N.W., Chen, J.M. 2007. Role of extracellular protein in the formation and stability of aerobic granules. *Enzyme and Microbial Technology*, **41**(5), 551-557.

[50] Zhang, Y.H., Dong, X.C., Liu, S., Lei, Z.F., Shimizu, K., Zhang, Z.Y., Adachi, Y., Lee, D.J. 2020. Rapid establishment and stable performance of a new algal-bacterial granule system from conventional bacterial aerobic granular sludge and preliminary analysis of mechanisms involved. *Journal of Water Process Engineering*, **34**, 101073.

List of figures

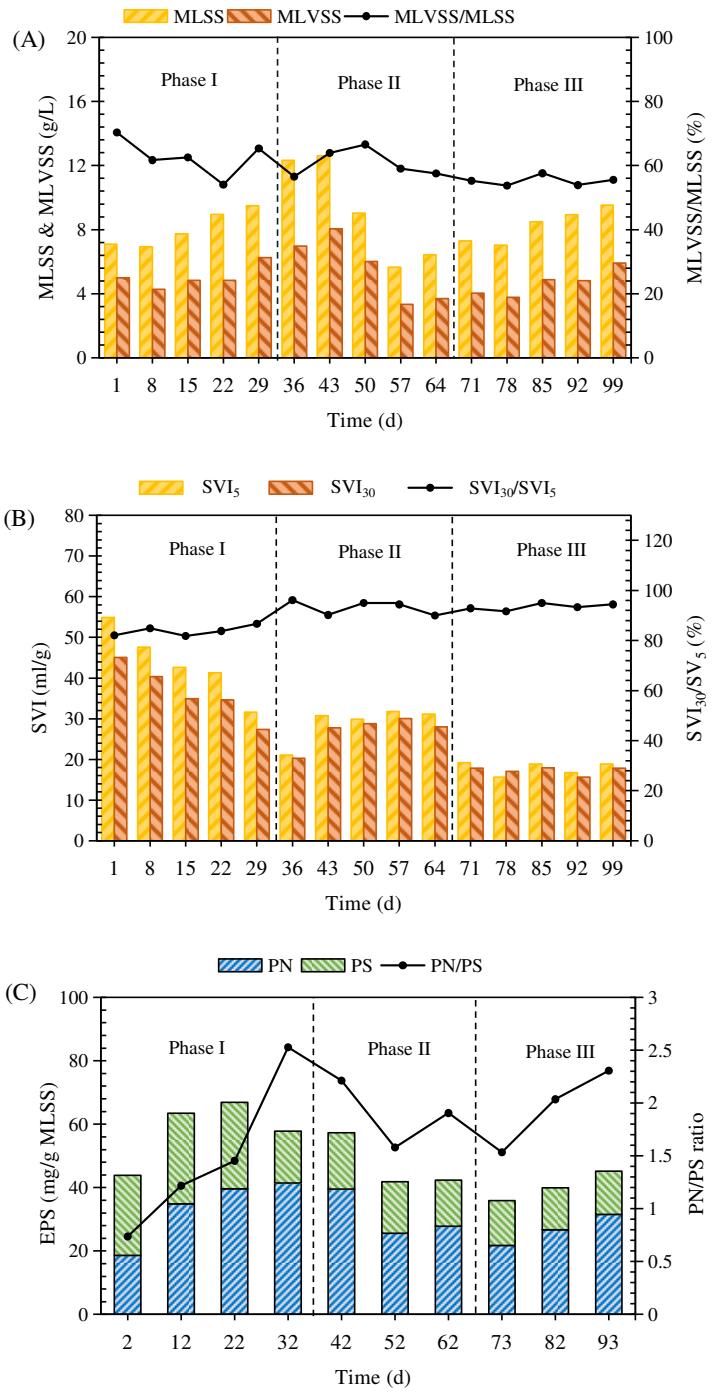

Fig. 1 Variations of ML(V)SS and MLVSS/MLSS (A), SVI_{30} and SVI_{30}/SVI_5 (B) and main EPS content, and PN/PS ratio (C) in three phases.

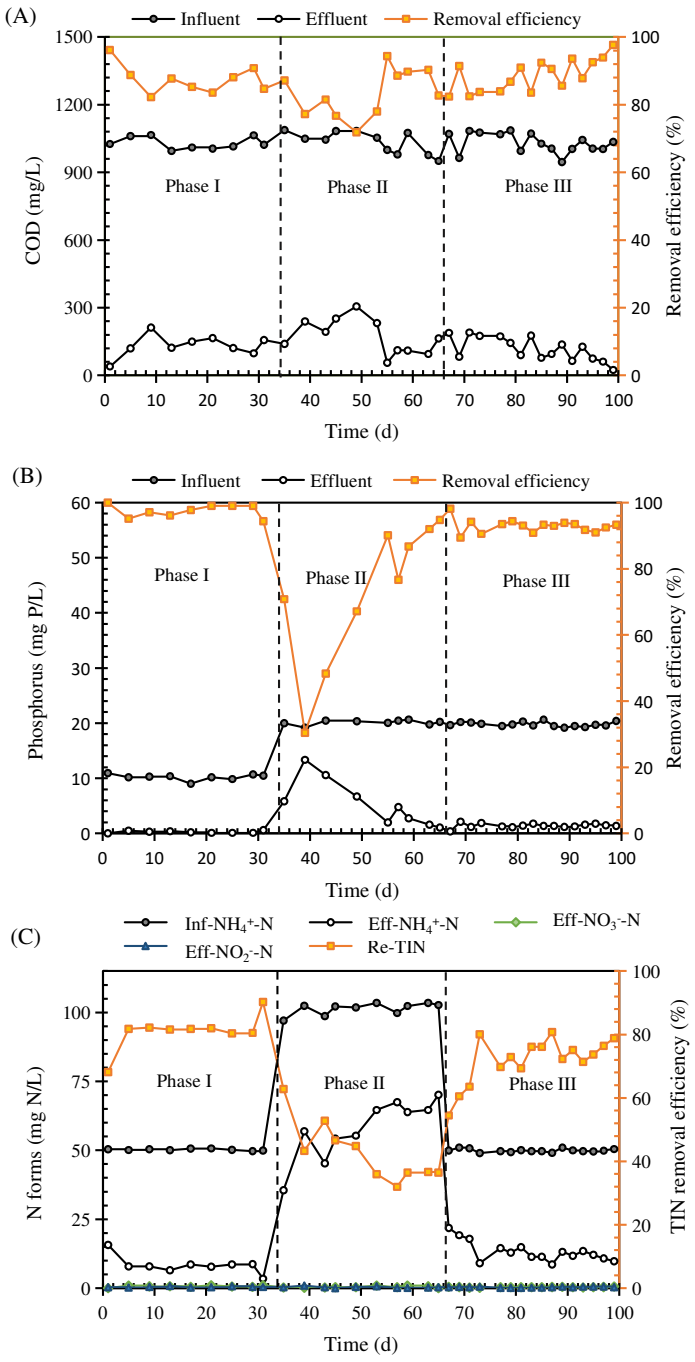

Fig. 2 Variation of COD (A), phosphorus (B) and nitrogen forms (C) during the whole experiment.

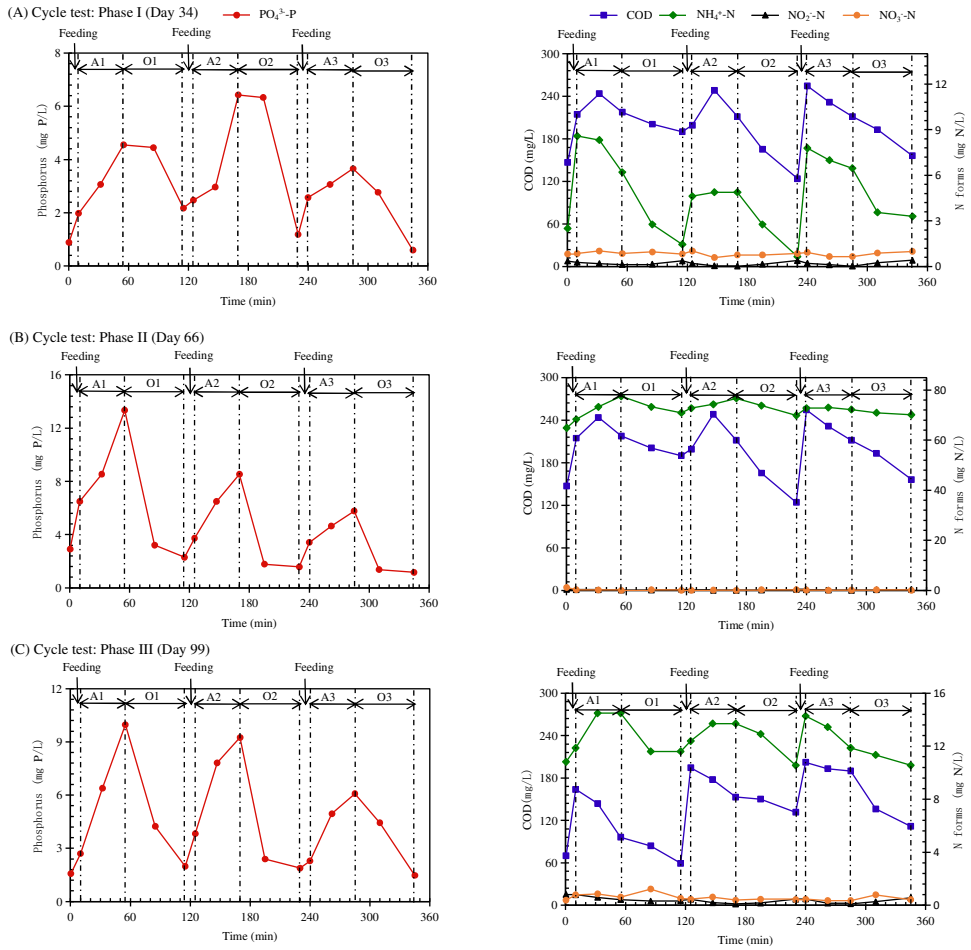

Fig. 3 Carbon, nitrogen, and phosphorus variation for one cycle on Day-34 (A), Day-66 (B) and Day-99 (C).

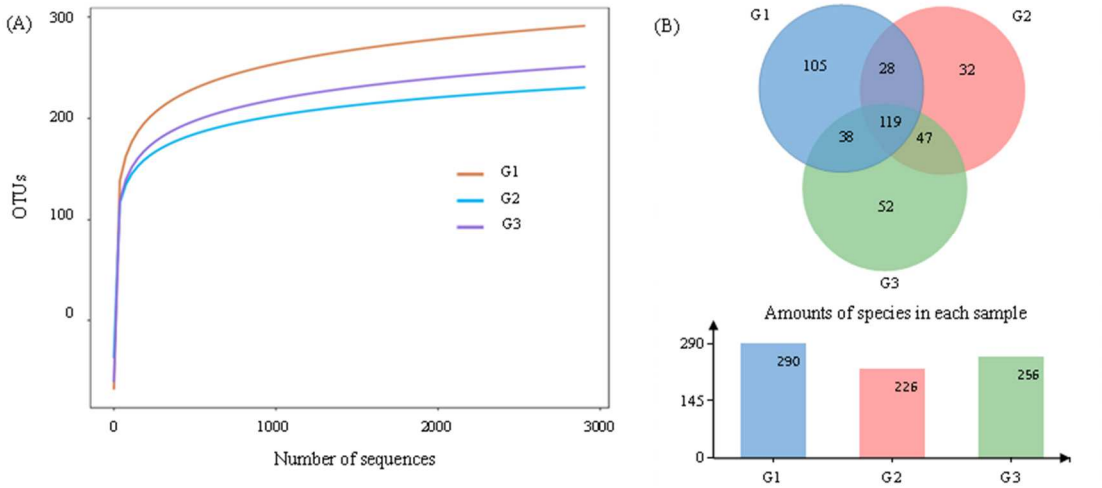

Fig. 4 Microbial community analysis of various samples in three phases: rarefaction curves for OTUs (A); Venn diagram of samples G1-G3 (B).

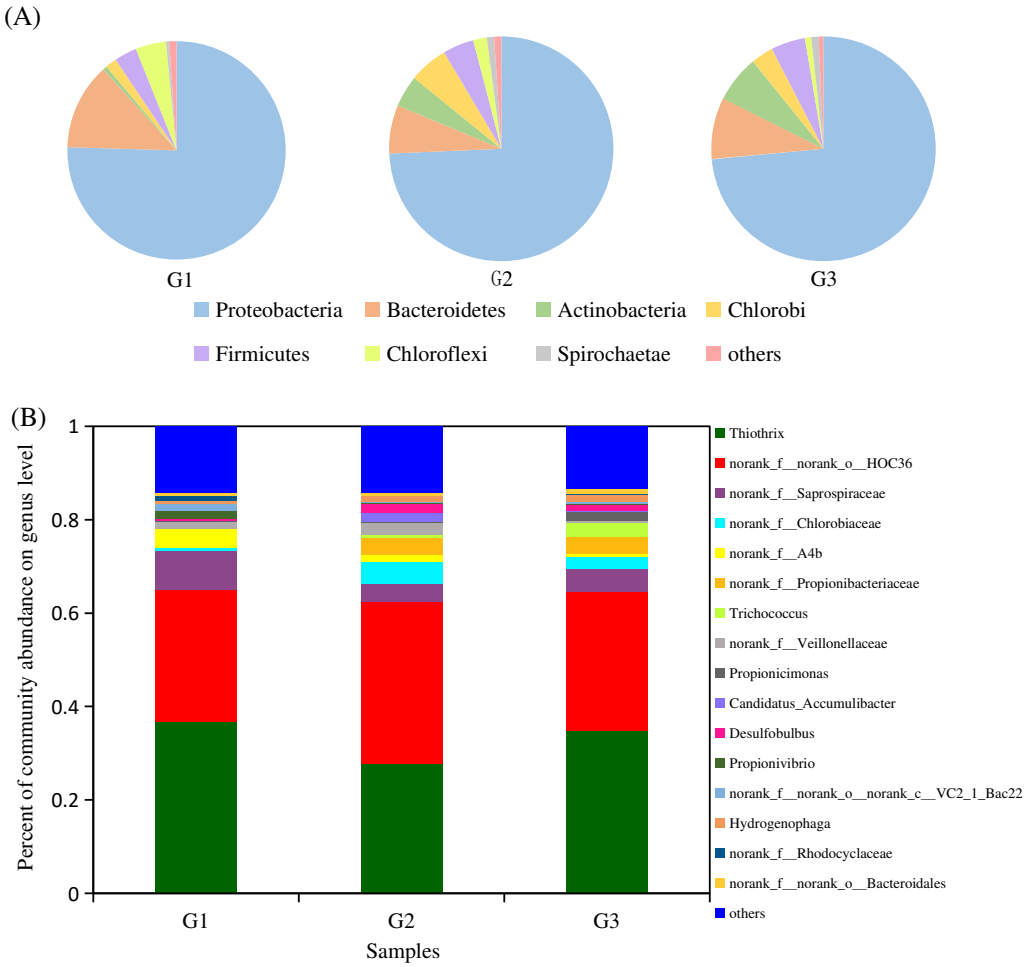

Fig. 5 Microbial community structures of samples G1-G3: bacterial community at the phylum (A) and genus (B) levels. Genera accounting for < 1% of the total composition of the community were classified as “others”.

List of tables

Table 1 Composition of the synthetic wastewater.

Components	Concentration (mg/L)	Trace elements [b]	Concentration (μg/L)
Glucose	330	$CoCl_2 \cdot 6H_2O$	250
Potassium acetate	540	$CuSO_4 \cdot 5H_2O$	250
Sodium propionate	300	$MnSO_4 \cdot H_2O$	250
$(NH_4)_2SO_4$ [a]	235, 470, 235	$NiCl \cdot 6H_2O$	250
K_2HPO_4 [a]	35, 70, 70		
KH_2PO_4 [a]	15, 30, 30		
$CaCl_2$	23		
$MgSO_4 \cdot 7H_2O$	22		
$FeSO_4 \cdot 7H_2O$	9		
$NaHCO_3$	100		

[a] These values were regularly increased according to the three periods (phase I, II, III)

[b] The micronutrient solution added in the synthetic wastewater were used for microbial growth.

Table 2 Feeding conditions during the whole experiment.

Phase	Time (day)	Organic loading rate (kg COD/L/d)	Nitrogen loading rate (mg N/L/d)	Phosphorus loading rate (mg P/L/d)	Ratio (COD: N: P)
Phase I	1–34	2.91 ± 0.10	146.54 ± 9.45	28.62 ± 1.46	100 : 5 : 1
Phase II	35–66	2.90 ± 0.13	288.97 ± 9.96	57.55 ± 2.26	100 : 10 : 2
Phase III	67–100	2.89 ± 0.12	138.37 ± 3.11	55.06 ± 1.51	100 : 5 : 2

Table 3 Species richness and diversity of G1, G2, and G3.

Samples	Effective reads	Observed OTUs	Community richness	Community diversity	
			Chao1[a]	Shannon[b]	Simpson[c]
G1	52,983	290	290	3.6663	0.78027
G2	45,500	226	226	3.8521	0.80049
G3	72,341	256	256.1	3.7781	0.79704

[a]A larger number → greater richness.

[b]A larger number → more diversity.

[c]A larger number → less diversity.

Table 4 Relative abundances of the key functional groups classification at genus level.

Key functional groups		Relative abundances (%)					
		G1		G2		G3	
AOB	*norank_f__Nitrosomonadaceae*	0.03		0.00		0.01	
NOB	*Nitrospira*	0.00	0.65	0.01	0.56	0.00	0.10
	norank_f__Xanthomonadaceae	0.57		0.55		0.10	
	norank_f__Pseudomonadaceae	0.08		0.00		0.00	
DNB	*Thiothrix*	36.84	38.88	27.69	30.49	34.85	37.82
	Zoogloea	0.01		0.19		0.12	
	Thauera	0.02		0.16		0.27	
	Rhodobacter	0.31		0.65		0.75	
	Chryseobacterium	0.06		0.00		0.01	
	Hydrogenophaga	0.63		1.23		1.44	
	Devosia	0.04		0.02		0.01	
	norank_f__Rhodospirillaceae	0.05		0.02		0.00	
	norank_f__Comamonadaceae	0.49		0.27		0.17	
	Rubrivivax	0.06		0.00		0.00	
	Paracoccus	0.00		0.09		0.07	
	Mesorhizobium	0.00		0.00		0.01	
	Acidovorax	0.09		0.09		0.03	
	Desulfovibrio	0.00		0.07		0.08	
	Pseudoxanthomonas	0.03		0.00		0.01	
	Flavobacterium	0.25		0.01		0.00	
PAOs	*Candidatus_Accumulibacter*	0.02	0.03	1.98	2.09	0.04	0.11
	Rhodococcus	0.00		0.00		0.01	
	Acinetobacter	0.01		0.11		0.06	
DNPAOs	*Dechloromonas*	0.03	0.43	0.06	0.56	0.02	0.43
	Aeromonas	0.15		0.07		0.07	
	Hyphomicrobium	0.08		0.37		0.34	
	Comamonas	0.17		0.06		0.00	
SRB	*Desulfomicrobium*	0.02	0.49	0.02	1.85	0.00	1.48
	Desulfobulbus	0.47		1.83		1.48	
SOB	*Thiobacillus*	0.03	0.07	0.00	0.54	0.02	3.13
	Trichococcus	0.04		0.54		3.11	